JOURNAL OF SOLID STATE CHEMISTRY 76, 319–327 (1988)

Substitutional Studies on the Anisotropic, Semiconducting, Molybdenum Bronze, $Li_{0.33}MoO_3$

B. T. COLLINS, K. V. RAMANUJACHARY, AND M. GREENBLATT*

Department of Chemistry, Rutgers, The State University of New Jersey, New Brunswick, New Jersey 08903

W. H. McCARROLL AND P. McNALLY

Department of Chemistry, Rider College, P.O. Box 6400, Lawrenceville, New Jersey 08648

AND J. V. WASZCZAK

A.T. & T., Bell Laboratories, Murray Hill, New Jersey 07974

Received February 25, 1988

Pure $Li_{0.33}MoO_3$ and vanadium-doped $Li_{0.33}Mo_{1-x}V_xO_3$ crystals were grown by a temperature gradient flux technique. Directional electrical resistivity measurements have been made on both the pure and doped crystals. The electrical properties of $Li_{0.33}MoO_3$ are highly anisotropic with resistivity values at room temperature of 1.8×10^{-1} and 6.0×10^2 Ω cm along the c and b^* directions, respectively. $Li_{0.33}MoO_3$ shows complex semiconducting behavior and an anomalously low paramagnetic signal. The effects of vanadium substitution on the structure and transport properties of $Li_{0.33}MoO_3$ are dramatic. Attempts are made to correlate the observed electrical and magnetic behavior with the structure of $Li_{0.33}MoO_3$.

Introduction

During the past few years considerable effort has been made to more fully characterize the alkali metal molybdenum oxide bronzes with respect to their electronic properties. Particular emphasis has been placed upon the phases with the general formula $A_{0.3}MoO_3$ (A = K, Tl, Rb), $A_{0.9}Mo_6O_{17}$ (A = Li, Na, K), and AMo_6O_{17} (A = Tl). All of these compounds exhibit highly anisotropic transport properties (*1–15*). $Li_{0.9}Mo_6O_{17}$ undergoes a superconducting transition at 1.9 K (*11*) while $Na_{0.9}Mo_6O_{17}$, $K_{0.9}Mo_6O_{17}$, $K_{0.3}MoO_3$, and $Rb_{0.3}MoO_3$ undergo charge-density wave (CDW) driven phase transitions (*1–7*). CDW-like transitions observed in $Li_{0.9}Mo_6O_{17}$, $TlMo_6O_{17}$, and $Tl_{0.3}MoO_3$ remain to be confirmed by low-temperature X-ray diffraction studies (*11, 13, 15*).

In contrast, bronzes with the formula $A_{0.33}MoO_3$ (A = Li, K, Cs) have not been studied to any great extent. This was due in part to the inability to grow well-formed crystals large enough for anything except

* To whom correspondence should be addressed.

0022-4596/88 $3.00

crystallographic studies (*16–20*). Strobel and Greenblatt have reported finding semiconducting behavior for the Li and Cs compounds on the basis of measurements made on small, ill-formed crystals obtained by fused salt electrolysis (*21*). Recently, the temperature gradient flux growth technique has been applied successfully for the growth of large single crystals of several molybdenum bronzes (*22, 23*), including $Li_{0.33}MoO_3$. The crystal structure of this triclinic phase (Fig. 1), which has been reported recently (*24*), is unlike that of the other bronzes which have Mo–O networks based upon ReO_3-like units. Rather, the $Li_{0.33}MoO_3$ structure contains V_2O_5-like layers in which lithium replaces every fourth transition metal in an ordered fashion. These layers are then linked by sharing edges and corners to yield an ideal compo-

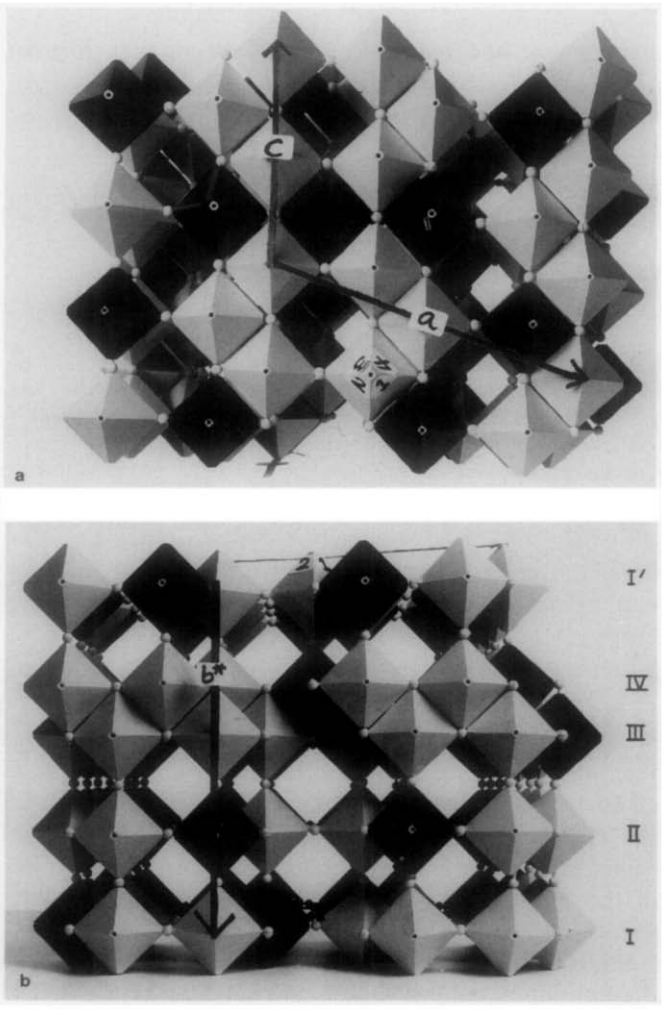

FIG. 1. (a) View along $\bar{b}^*$ of the $Li_{0.33}MoO_3$ structure built from idealized MoO_6 (light) and LiO_6 (dark) octahedra showing the V_2O_5-like planes. (b) View along c of the $Li_{0.33}MoO_3$ structure showing the V_2O_5-like layers connected along b^* (vertical direction) to form the three-dimensional structure.

sition of $LiMo_3O_9$, or in keeping with the more traditional bronze-like formulation, $Li_{0.33}MoO_3$. Along the c direction, MoO_6 octahedra are connected by corner-sharing to form infinite chains; the Mo–O bond distances are sufficiently short (1.861–1.995 Å) for good Mo–O–Mo dt_{2g}-$p\pi$ orbital overlap. Along b^*, the Mo–O–Mo interactions arise from corner- and edge-sharing octahedra; however, some of the Mo–O distances (which vary between 1.660 and 2.400 Å) are too long for effective orbital overlap. In other directions of the crystal Mo–O–Mo interactions are not continuous. The structure, although three-dimensional overall, is anisotropic with respect to the Mo–O bonding which should be a prime factor in determining the electronic properties of this material. Chemical analysis of several different samples of this compound shows that the lithium content deviates little, if any (i.e., $<\pm 1\%$ mole) from the ideal stoichiometry (*22*).

Schneemeyer and co-workers (*8–10*) showed that tungsten can replace molybdenum by up to 12 mole% in $K_{0.3}MoO_3$ and that considerably smaller amounts markedly alter the electronic properties of this compound, including loss of metallic behavior. Similar effects have been shown to occur in $Li_{0.9}Mo_6O_{17}$ (*25*) and $K_{0.9}Mo_6O_{17}$ (*26*). Although these three compounds are metallic at room temperature, while $Li_{0.33}MoO_3$ is semiconducting, the highly anisotropic nature of the Mo–O network and the possibility that its electronic properties might be modified by vanadium substitution, seemed to warrant further investigation now that suitable single-crystal specimens were available. It has been shown recently that tungsten substitution favors the growth of $Li_{0.9}Mo_{6-x}W_xO_{17}$ crystals by the temperature gradient flux growth method (*25*) and although tungsten can replace molybdenum in $Li_{0.33}MoO_3$ to some extent, the latter product is obtained in microcrystalline form only. In contrast, the results of this experiment show that the presence of vanadium favors the growth of $Li_{0.33}Mo_{1-x}V_xO_3$ and suppresses the growth of $Li_{0.9}Mo_6O_{17}$. The results of the synthetic and subsequent electrical and magnetic studies are reported here.

Experimental

Conditions for the synthesis of the vanadium-substituted phases were the same as those described previously for the preparation of pure $Li_{0.33}MoO_3$ except for the differences noted below. The reactants were weighed out to the nearest milligram according to the following equation,

$$(y + z)Li_2MoO_4 + (2 - 2z - 3y)MoO_3 + zMoO_2 + yV_2O_5 = 2Li_{y+z}Mo_{1-y}V_yO_3,$$

where $y + z = 0.35$–0.50 and $y = 0$–0.20. A 3-day preheat of the 10-g charge was carried out at 565°C followed by 7 days under temperature gradient conditions with the hot zone set at 637(±3)°C and the cold zone at 582(±3)°C over a 15-cm length (see (*23*) for details). All reagents were as described previously with the V_2O_5 also being of reagent grade. Crystals of $Li_{0.33}Mo_{1-x}V_xO_3$ grow in the cold zone, their size and quality depending upon the initial stoichiometry as is discussed subsequently.

The phases formed were routinely identified by X-ray powder diffractometry using nickel-filtered copper radiation. Lattice parameters were obtained by least-squares refinement of selected reflections up to $2\theta = 55°$. The orientation of selected crystals used for resistivity measurements was confirmed by Weissenberg and precession photography. Chemical analysis for Li, Mo, and V were performed using a Spectrometrics DC plasma emission spectrometer and are nominally considered accurate to ±2%.

Low-temperature electrical resistivity measurements were made with a four-probe configuration using ultrasonically soldered indium contacts in a conventional

liquid helium cryostat. It should be noted that for all resistivity measurements, data was no longer collected when the sample resistance exceeded $1 \times 10^5\ \Omega$. High temperature measurements (up to 700 K) also employed a four-probe technique by attaching thin platinum wires with Acheson Electrodag 154. The samples were measured in a quartz cell under vacuum. The largest error in the resistivity data is about 25%. A DuPont Instruments 9900 thermal analysis system was used for DSC measurements. Magnetic susceptibilities were measured by the Faraday method.

Results and Discussion

Synthesis

The growth of crystals of $Li_{0.33}Mo_{1-x}V_xO_3$ appears to be optimized for initial charge compositions between $Li_{0.35}MoO_3$ and $Li_nMo_{1-y}V_yO_3$ for n between 0.35 and 0.45 and for y between 0.0 and 0.10. Within these ranges, crystals 3–5 × 0.5 × 0.5 mm^3 are not uncommon while some are found up to 1 cm long. For $y \geq 0$ and $n \geq 0.35$, the formation of $Li_{0.9}Mo_6O_{17}$ is effectively suppressed. Although this phase is present, the crystals are ill-formed and are concentrated in the hot zone for $n = 0.35$. However, for $n = 0.35$ and $y = 0$, $Li_{0.9}Mo_6O_{17}$ is the dominant phase and is found in the cold zone as well-formed crystals (*22*). Above $y = 0.10$, the size of the crystallites falls off markedly. A small amount of microcrystalline material can be obtained at $y = 0.15$. At $y = 0.20$, the washed products are biphasic powders with the primary phase being a solid solution of VO_2 and MoO_2.

The chemical formulae of several representative phases, as determined by chemical analysis, are given in Table I and indicate that the vanadium substitution takes place up to at least 8.5 mole%. It may perhaps be higher in the biphasic material which was not analyzed. The variation in the lithium content is somewhat above that expected for the analytical technique and may indicate a small range of nonstoichiometry in these materials.

Crystals of $Li_{0.33}MoO_3$ are commonly found with an elongated plate-like habit, the plate surface being in the *ac* plane of the crystal. These crystals are characterized by easy cleavage parallel to this plane. Although the structure is three-dimensional overall, the Mo–O bond distances show significant variations (*24*). Fifteen of the 72 unique Mo–O distances in the various MoO_6 octahedra are quite long: 2.31–2.71 Å. Twelve of these 15 distances are approximately perpendicular to the *ac* plane and thus the observed cleavage is not unex-

TABLE I

CRYSTAL COMPOSITIONS AND LATTICE PARAMETERS FOR $Li_{0.33}Mo_{1-x}V_xO_3$

Sample	Charge composition	Crystal composition	*a* (Å)	*b* (Å)	*c* (Å)	α (°)	β (°)	γ (°)	*V* (Å^3)
II-106A	$Li_{0.40}MoO_3$	$Li_{0.32}MoO_3$[a]	13.079(2)	15.453(2)	7.476(1)	96.97(2)	106.56(2)	103.37(9)	1380.4(9)
II-106A	$Li_{0.40}MoO_3$	$Li_{0.32}MoO_3$[a]	13.093(5)	15.453(4)	7.477(2)	96.97(5)	106.66(6)	103.38(3)	1380.9(5)
III-9	$Li_{0.50}MoO_3$	$Li_{0.32}MoO_3$[a]	13.083(6)	15.456(6)	7.476(6)	97.03(6)	106.52(6)	103.46(4)	1380.5(8)
I-10/55	$Li_{0.40}MoO_3$		13.080(6)	15.450(3)	7.477(3)	96.88(5)	106.55(7)	103.41(2)	1380.7(7)
VIII-33	$Li_{0.35}Mo_{0.99}V_{0.01}O_3$	$Li_{0.34}Mo_{0.974}V_{0.026}O_3$	13.103(8)	15.441(6)	7.476(6)	96.85(7)	106.69(9)	103.47(4)	1380.1(7)
III-75c	$Li_{0.35}Mo_{0.95}V_{0.05}O_3$	$Li_{0.33}Mo_{0.948}V_{0.052}O_3$	13.083(5)	15.388(4)	7.474(2)	96.85(6)	106.62(6)	103.48(3)	1373.8(5)
I-56	$Li_{0.40}Mo_{0.95}V_{0.05}O_3$	$Li_{0.31}Mo_{0.942}V_{0.058}O_3$	13.094(7)	15.364(5)	7.470(3)	97.00(9)	106.72(7)	103.47(3)	1370.5(8)
I-58	$Li_{0.50}Mo_{0.90}V_{0.10}O_3$	$Li_{0.31}Mo_{0.933}V_{0.067}O_3$	13.081(6)	15.346(6)	7.470(3)	97.00(8)	106.59(8)	103.52(4)	1368.3(7)
III-96	$Li_{0.35}Mo_{0.90}V_{0.10}O_3$	$Li_{0.34}Mo_{0.929}V_{0.071}O_3$	13.074(6)	15.352(4)	7.469(2)	97.03(6)	106.61(6)	103.54(5)	1367.4(5)
I-54	$Li_{0.40}Mo_{0.85}V_{0.15}O_3$	$Li_{0.32}Mo_{0.915}V_{0.085}O_3$	13.079(8)	15.298(5)	7.461(3)	96.58(11)	106.63(12)	103.64(5)	1363.1(8)

[a] From Ref. (*22*).

pected. Substitution of vanadium for molybdenum results in a decrease of the unit cell volume which is to be expected when vanadium(IV) or (V) replaces molybdenum(V). However, the shrinkage is unexpectedly large for the amount of vanadium that is added with the principal change being a marked drop in the length of the *b* parameter from 15.45 Å for pure $Li_{0.33}MoO_3$ to 15.30 Å for $Li_{0.32}Mo_{0.915}V_{0.085}O_3$ as shown in Table I.

Whether or not it is a fortuitous circumstance of our experimental conditions, it is interesting to note that the observed limit for vanadium substitution corresponds to 1 in 12 molybdenums. However, based on bond length–bond strength calculations for the pure compound (*24*) there appears to be no one site that is particularly favored electrostatically for pentavalent substituents. Rather, there are four octahedra which appear particularly favorable for hexavalent substitutions while the remaining eight have average Mo valences between 5.54 and 5.69. Clearly, the exact nature of this substitution will have to be answered by a structural study. It also is noteworthy that the ease of cleavage appears to decrease as vanadium is added to the crystal and that the habit becomes more needle-like rather than plate-like.

Electrical and Magnetic Properties

Pure $Li_{0.33}MoO_3$ exhibits semiconducting temperature dependence between 105 and 700 K. The Arrhenius plot of the resistivity from room temperature to 105 K for crystals grown by the temperature gradient flux technique (TGFT) is shown in Fig. 2. The data shows similar temperature dependence as that found for crystals prepared by molten salt electrolysis (*21*). Activation energies can be approximated from Fig. 2. Values of 0.27 and 0.01 eV have been found in the temperature ranges 298 to 180 K and 125 to 105 K, respectively, for current passed along *c*. On another crystal of $Li_{0.33}MoO_3$, the temperature dependence along *b** has been measured. Between 298 and 205 K an activation energy of 0.23 eV has been calculated. A comparison of the data for measurements along *c* and *b** is shown in Fig. 2 (inset). The anisotropic nature of $Li_{0.33}MoO_3$ is evident when one compares room temperature resistivity values obtained along *c* and *b**. The value of ρ_c (298 K), 1.8×10^{-1} Ω cm, is more than three orders of magnitude less than that found for ρ_{b^*} (298 K), 6.0×10^2 Ω cm. This result is consistent with the structure of $Li_{0.33}MoO_3$ since the Mo–O $p\pi$ overlap should be much better along *c* than *b** (*24*).

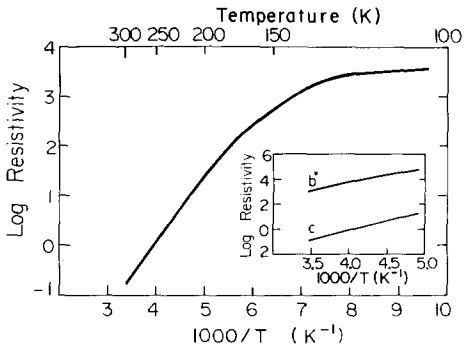

FIG. 2. Log resistivity vs 1000/*T* for $Li_{0.33}MoO_3$ for current along *c* between 298 and 105 K. Inset: comparison of the data along *c* and *b** for $Li_{0.33}MoO_3$.

We have also measured the temperature dependence of the resistivity for various vanadium-substituted single crystals. Crystal morphology precluded measurement along any crystallographic direction except *c*. Table II lists room-temperature resistivity values along with activation energies. For 2.6 mole% vanadium doping, the room-temperature resistivity increases by an order of magnitude. The activation energies, E_{a_1} and E_{a_2}, are 0.25 and 0.22 eV from 298 to 210 K and 200 to 180 K, respectively. Further vanadium substitution (5.8 mole%) continues to increase the room-temperature resistivity. Activation energies of 0.22 and 0.19 eV are estimated from 298 to 225 K

TABLE II

RESISTIVITY VALUES AND ACTIVATION ENERGIES FOR $Li_{0.33}Mo_{1-x}V_xO_3$

Sample	Current	Crystal composition	ρ (298 K) Ω cm	E_{a_1} (eV)	E_{a_2} (eV)
I-10	c	$Li_{0.33}MoO_3$	1.8×10^{-1}	0.27	0.01
I-10	b^*	$Li_{0.33}MoO_3$	6.0×10^{2}	0.23	
VIII-33	c	$Li_{0.34}Mo_{0.974}V_{0.026}O_3$	1.8	0.25	0.22
I-56	c	$Li_{0.31}Mo_{0.942}V_{0.058}O_3$	3.7	0.22	0.19
III-96	c	$Li_{0.34}Mo_{0.929}V_{0.071}O_3$	7.3×10^{-1}	0.22	
III-96	c	$Li_{0.34}Mo_{0.929}V_{0.071}O_3$	8.3×10^{-1}	—	—

and 210 to 170 K, respectively. Substitution of 7.1 mole% vanadium results in a decrease of the resistivity although pure $Li_{0.33}MoO_3$ is still more conducting. In Table II, results of the room-temperature resistivities of two different crystals from the same preparation (III-96) suggest that the decrease in the resistivity of the V-doped sample is real (i.e., the difference between I-10c and VIII-33c in Table II is greater than the experimental error of measurement indicated by the measurements on two III-96c samples). From Fig. 3 it can be observed that between 298 and 160 K, $Li_{0.34}Mo_{0.929}V_{0.071}O_3$ has a single activation energy of 0.22 eV. Closer examination of Fig. 3 reveals that crystals of $Li_{0.33}Mo_{1-x}V_xO_3$, where $x = 0$, 0.026, and 0.058, do not follow the usual linear log ρ vs T^{-1} dependence; however, when $x = 0.071$ linear behavior is observed down to 160 K. When $x = 0.026$ and 0.058 the amount of nonlinearity is less than that found for pristine $Li_{0.33}MoO_3$. V-doped samples were not measured at lower temperatures due to the high resistance of the samples. Therefore, it could not be determined if the substituted crystals show a saturated behavior, as is found for $Li_{0.33}MoO_3$, at lower temperatures.

Resistivity measurements on $Li_{0.33}MoO_3$ for current along c between room temperatures and 700 K (Fig. 4) show evidence of a broad transition near 360 K. The activation energy between 298 and 318 K is 0.27 eV. Above the transition, $Li_{0.33}MoO_3$ appears to behave as a simple thermally activated semiconductor with $E_a = 0.12$ eV from 317 to 600 K.

The magnetic susceptibility data for non-oriented single crystals of $Li_{0.33}MoO_3$ and $Li_{0.31}Mo_{0.942}V_{0.058}O_3$ with the contribution from paramagnetic impurities subtracted out is shown in Fig. 5. The very weak paramagnetic signal for $Li_{0.33}MoO_3$ follows Curie behavior between 300 and 50 K. Below ~50 K there is a broad transition with a maximum at 25 K. At lower temperatures a Curie tail is observed. $Li_{0.31}Mo_{0.942}V_{0.058}O_3$ is diamagnetic. The anomaly near 55 K is of unknown origin. The diamagnetic signal is consistent with a d^0 ion, vanadium(V), sub-

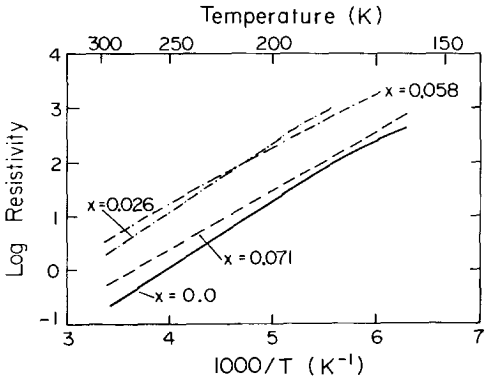

FIG. 3. Log resistivity vs $1000/T$ for $Li_{0.33}Mo_{1-x}V_xO_3$ for current along c between 298 and 160 K.

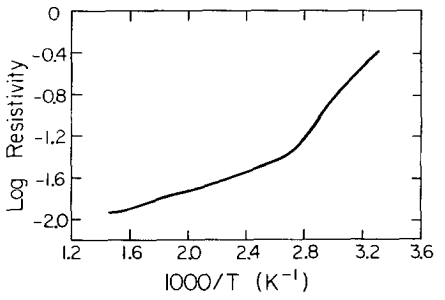

FIG. 4. Log resistivity vs $1000/T$ for $Li_{0.33}MoO_3$ for current parallel with c between 298 and 700 K.

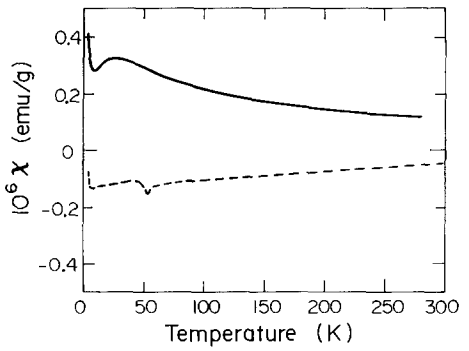

FIG. 5. Magnetic susceptibility vs temperature for randomly oriented crystals of $Li_{0.33}MoO_3$ (solid line) and $Li_{0.31}Mo_{0.942}V_{0.058}O_3$ (dashed line) between 4.2 and 300 K.

stituting for a d^1 ion, molybdenum(V). This result, coupled with the V_2O_5-like structure of $Li_{0.33}MoO_3$, can be used to argue that in the V-doped compounds at least a majority, if not all, of the V ions are in the pentavalent state.

The transport properties of $Li_{0.33}MoO_3$ are unique in the class of materials called molybdenum oxide bronzes. Its anomalous electrical and magnetic behavior cannot be explained by arguments similar to that applied to the other reduced compounds. Although its stoichiometry is the same as that found for the red bronzes, $A_{0.33}MoO_3$ where A = K, Rb, Cs, the structure and transport properties are markedly different. The red bronzes have room temperature resistivity values on the order of 10^4–10^5 Ω cm, as compared to ~0.2 Ω cm for $Li_{0.33}MoO_3$ and display typical semiconducting behavior with activation energies ~0.1 eV.

The behavior of $Li_{0.33}MoO_3$ is quite complex. The pyrochlore compounds $Ln_2Mo_2O_7$, where Ln = Y, Tb, show similar nonlinear $\log \rho$ vs T^{-1} dependence (*27*). However, it should be noted that these pyrochlore materials are much better conductors than $Li_{0.33}MoO_3$. In addition, highly doped metal oxide semiconductors such as $Li_xNi_{1-x}O$ (*28*) and semimetallic alloys like Bi–Sb (*29*) also show qualitatively the same behavior. A hopping conduction was invoked to explain the behavior in $Li_xNi_{1-x}O$ while impurity band formation was used to describe the properties of the Bi–Sb alloys.

Qualitative Seebeck measurements on $Li_{0.33}MoO_3$ and $Li_{0.31}Mo_{0.942}V_{0.058}O_3$ near room temperature reveal p-type majority carriers for both samples. It appears that $Li_{0.33}MoO_3$ is an extrinsic semiconductor with acceptor levels lying close in energy to the valence band. A small deficiency of Li^+ ions might lead to the introduction of such impurity levels. The resistivity and Seebeck measurements are consistent with the band structure calculations of Canadell and Whangbo (*30*) which predict $Li_{0.33}MoO_3$ to be a small band gap semiconductor. In this scheme it is possible to have very few free electrons present. This could account for the anomalously low paramagnetic signal in $Li_{0.33}MoO_3$. ESR measurements on $Li_{0.33}MoO_3$ by Strobel and Greenblatt (*21*) show the presence of unpaired d^1 electrons at low temperature. However, no conclusions were made due to the poor quality of the spectra.

The correlation of the resistivity along the crystallographic c direction as a function of x for the $Li_{0.33}Mo_{1-x}V_xO_3$ crystals is difficult to interpret due to the complexity of the structure. As stated earlier, the room-temperature resistivity increases 20-fold with 5.8 mole% vanadium substitution. From Table I it can be observed that the c cell parameter decreases only ~0.007 Å with this level of doping. It is believed that the vanadium disrupts the Mo–O overlap along c. The subsequent decrease of the resistivity for the 7.1 mole% V-doped sample is surprising. In addition, the observation of a linear $\log \rho$ vs T^{-1} dependence from room temperature to 160 K is an unexpected result. It is possible that the high level of V-doping distorts the structure of $Li_{0.33}MoO_3$ which, in turn, alters the band structure. This claim needs to be investigated further.

The broad transition seen in the electrical resistivity of $Li_{0.33}MoO_3$ has been investigated by other measurements. There was no evidence of the 360 K transition in either the DSC or high-temperature X-ray powder diffraction data. Presumably some small structural changes occur which alter the electronic structure of $Li_{0.33}MoO_3$ dramatically. Although ionic effects, i.e., increased lithium ion mobility, are not likely to dominate the behavior due to the large electrical conductivity, it should be noted that there are empty channels in the structure of $Li_{0.33}MoO_3$ along the *c* direction which might facilitate fast ionic motion.

In summary, $Li_{0.33}MoO_3$ is an unusual triclinic molybdenum oxide bronze which is structurally derived from V_2O_5-like layers in contrast to the other Mo bronzes whose structures are based on ReO_3-like corner-sharing octahedra. Along *c*, MoO_6 octahedra are connected by corner-sharing to form infinite chains and the Mo–O bond distances are sufficiently short for good Mo–O–Mo dt_{2g}-$p\pi$ orbital overlap. Experimentally, the highest conductivity has been measured in this direction. Along b^*, the Mo–O–Mo interactions arise from corner- and edge-sharing octahedra. However, the range of Mo–O bond lengths is wide and some of these distances are too long for good orbital overlap. As predicted by the structure, the resistivity along b^* was found to be orders of magnitude greater than along *c*. Qualitative Seebeck measurements on $Li_{0.33}MoO_3$ indicate *p*-type semiconducting behavior. Acceptor levels lying close in energy to the valence band have been invoked to explain the observed electronic and magnetic transport properties. This is in agreement with the resistivity data and theoretical calculations (*30*) which indicate small band gap semiconducting properties.

It was previously suggested (*24*) that along *c* $Li_{0.33}MoO_3$ might be a metallic conductor. Nevertheless, although the conductivity is quite good $(\sim 5\ \Omega\ cm)^{-1}$ at room temperature), semiconducting behavior is observed. Some experiments which could help clarify the properties of $Li_{0.33}MoO_3$ are: (1) directional magnetic susceptibility, (2) single-crystal X-ray studies of the V-doped samples, (3) the effects of substituting other elements, if possible, and (4) Seebeck and/or Hall coefficient measurements to determine the carrier type as a function of temperature.

Acknowledgments

We thank Professor F. J. DiSalvo for useful discussions and Professor M.-H. Whangbo for providing a preprint of his article on the band calculation of $Li_{0.33}MoO_3$. We are grateful to Nancy Brown of the Geology Department at Princeton University for the high-temperature X-ray diffraction measurements. This work received support from the National Science Foundation Solid State Chemistry Grant DMR-84-04003 and National Science Foundation Materials Research Instrumentation Grant DMR-84-08266. W.H.M. and P.M. are grateful for support under NSF DMR-87-02034.

References

1. R. Buder, J. Devenyi, J. Marcus, J. Mercier, C. Schlenker, and H. Vincent, *J. Phys. Lett.* **43,** L-59 (1982).
2. C. Escribe-Filippini, K. Konate, J. Marcus, C. Schlenker, R. Almairac, R. Ayroles, and C. Roucau, *Philos. Mag. B* **50,** 321 (1984).
3. J. P. Pouget, J. Kagoshima, C. Schlenker, and J. Marcus, *J. Phys. Lett.* **44,** L-113 (1987).
4. E. Bervas, R. W. Cochrane, J. Dumas, C. Escribe-Filippini, J. Marcus, and C. Schlenker, "Charge Density Waves in Solids," Lecture Notes in Physics, Vol 17, p. 144, Springer-Verlag, Berlin (1985).
5. C. Schlenker, J. Dumas, C. Escribe-Filippini, H. Guyot, J. Marcus, and G. Fourcadot, *Philos. Mag. B* **52,** 643 (1985).
6. C. Schlenker and J. Dumas, *in* "Crystal Chemistry and Properties of Materials with Quasi-One-Dimensional Structures" (J. Rouxel, Ed.), p. 135, Reidel, Dodrecht (1985).
7. R. M. Fleming and L. F. Schneemeyer, *Phys. Rev. B* **28,** 6996 (1983).
8. L. F. Scheemeyer, F. J. DiSalvo, S. E. Spengler, and J. V. Waszczak, *Phys. Rev. B* **30,** 4297 (1984).

9. L. F. SCHNEEMEYER, S. F. SPENGLER, F. J. DISALVO, AND J. V. WASZCZAK, *Mol. Cryst. Liq. Cryst.* **125,** 41 (1985).
10. R. J. CAVA, L. F. SCHNEEMEYER, R. M. FLEMING, P. B. LITTLEWOOD, AND E. A. RIETMAN, *Phys. Rev. B* **32,** 4088 (1985).
11. M. GREENBLATT, W. H. MCCARROLL, R. NEIFELD, M. CROFT, AND J. V. WASZCZAK, *Solid State Commun.* **51,** 671 (1984).
12. M. GREENBLATT, K. V. RAMANUJACHARY, W. H. MCCARROLL, R. NEIFELD, AND J. V. WASZCZAK, *J. Solid State Chem.* **59,** 149 (1985).
13. B. T. COLLINS, K. V. RAMANUJACHARY, M. GREENBLATT, AND J. V. WASZCZAK, *Solid State Commun.* **56,** 1023 (1985).
14. M. GANNE, A. BOUMAZA, M. DION, AND J. DUMAS, *Mater. Res. Bull.* **20,** 1297 (1985).
15. K. V. RAMANUJACHARY, B. T. COLLINS, M. GREENBLATT, AND J. V. WASZCZAK, *Solid State Commun.* **59,** 647 (1986).
16. A. WOLD, W. KUNNMANN, R. J. ARNOT, AND A. FERRETTI, *Inorg. Chem.* **3,** 545 (1964).
17. A. F. REID AND J. A. WATTS, *J. Solid State Chem.* **2,** 16 (1970).
18. N. C. STEPHENSON AND A. D. WADSLEY, *Acta Crystallogr.* **19,** 241 (1965).
19. J. M. REAU, C. FOUASSIER, AND P. HAGENMULLER, *J. Solid State Chem.* **1,** 326 (1970).
20. J. M. REAU, C. FOUASSIER, AND P. HAGENMULLER, *Bull. Soc. Chem. Fr.,* 2883 (1971).
21. P. STROBEL AND M. GREENBLATT, *J. Solid State Chem.* **36,** 331 (1981).
22. W. H. MCCARROLL AND M. GREENBLATT, *J. Solid State Chem.* **54,** 282 (1984).
23. K. V. RAMANUJACHARY, M. GREENBLATT, AND W. H. MCCARROLL, *J. Cryst. Growth* **70,** 476 (1985).
24. P. P. TSAI, J. A. POTENZA, M. GREENBLATT, AND H. J. SCHUGAR, *J. Solid State Chem.* **64,** 47 (1986).
25. K. V. RAMANUJACHARY, B. T. COLLINS, M. GREENBLATT, P. MCNALLY, AND W. H. MCCARROLL, *Solid State Ionics* **22,** 105 (1986).
26. J. DUMAS, C. ESCRIBE-FILIPPINI, J. MARCUS, J. MERCIER, D. SALOMON, C. SCHLENKER, AND F. RAZAVI, *Physica* **117–118,** 602 (1983).
27. J. E. GREEDAN, M. SATO, N. ALI, AND W. R. DATARS, *J. Solid State Chem.* **68,** 300 (1987).
28. A. J. SPRINGTHORPE, I. G. AUSTIN, AND B. A. AUSTIN, *Solid State Commun.* **3,** 143 (1965).
29. A. L. JAIN, *Phys. Rev.* **114,** 1518 (1959).
30. E. CANADELL AND M.-H. WHANGBO, *Inorg. Chem.* **27,** 228 (1988).